State and Parameter Estimation of a Neural Mass Model from Electrophysiological Signals during Induced Status Epilepticus

Armando López–Cuevas, Bernardino Castillo–Toledo, Laura Medina–Ceja, and Consuelo Ventura–Mejía

Centro de Investigación y de Estudios Avanzados del Instituto Politécnico Nacional, CINVESTAV, Unidad Guadalajara
Av. del Bosque 1145, Col. El Bajío, Zapopan, 45015, Jalisco, México

Laboratorio de Neurofisiología y Neuroquímica, Departamento de Biología Celular y Molecular, CUCBA, Universidad de Guadalajara, México
{acuevas,toledo}@gdl.cinvestav.mx

Abstract. Epilepsy is a brain disorder characterized by transitions from normal (interictal) activity to seizure activity (ictal). These transitions are unpredictable and little is known about the mechanisms that triggers them. In this article we use a computational modelling approach combined with in vivo electrophysiological data obtained from pilocarpine model of epilepsy to infer about changes that may lead to a seizure, special emphasis is done in analyzing parameters changes during or after pilocarpine administration. A cubature Kalman filter is utilized to estimate parameters and states of the model in real time from the observed electrophysiological signal.

Keywords: Cubature Kalman Filter, Epilepsy, Neural Mass Model, Pilocarpine, Population Model, Real Time Parameter and States Estimation, Status Epilepticus.

1 Introduction

Epilepsy is a brain disorder characterized by recurrent seizures affecting 2-5% of world's population. Seizures are generated by abnormal, hypersynchronic neuronal activity in the brain; its onset can involve several regions (generalized seizures) or just a circumscribed brain region (focal seizures) [1]. The causes of epilepsy are multifactorial, among the known causes there are infections, injuries, abnormal brain development, unbalance in neurotransmitters, brain tumors and others. Epilepsy treatments include pharmacology or surgical methods but even with advances in medicine approximately 30% of patients remain with seizures [2]. If there were a way to estimate internal changes that lead to seizures then it would be possible to design devices able to deliver drugs or electrical stimulation automatically in real time in order to reduce or abolish such pathological activity, even more, if one can account with a model that describes the electrical

activity in a certain region in the brain then a feedback control strategy could be designed to maintain activity within normal behavior.
Computational modelling in neuroscience is a well-established and increasing research area that has helped to better understand mechanisms underlying certain brain activity or phenomena. When combined with experimental studies it can be a powerful tool in brain research, especially in brain disorders [3, 4]. In this work, we use neural mass modelling [5] combined with in-vivo experiments to investigate whether a change in the states and parameters of the model can be observed during the transition to *status epilepticus* (SE). By using a cubature Kalman filter (CKF) [6] we are able to jointly estimate states and parameters changes on-line.
The article is organized as follows: In section II, the experimental methods carried out for data acquisition are described along with the animal model of epilepsy used in this study; in section III the electrophyiological signals are analyzed in frequency domain and differences between interictal and ictal signals are remarked; section IV introduces the neural mass models and in section V a description of the model used here is given, and then, signals produced by the model are compared to the real signals. In section VI we present state and parameter identification from electrophysiological signals, finally, section VII presents results and conclusions.

2 Experimental setting

2.1 Pilocarpine model of epilepsy

Pilocarpine is a muscarinic agonist used to reproduce several characteristics present in human temporal lobe epilepsy. This experimental model was chosen because the electrophysiological activity of animal models that were administered pilocarpine resembles to that in human temporal lobe epilepsy [7].

Male Wistar rats (190-200 g) were maintained individually in a temperature controlled room (22 2C) on a 12 h light/dark cycle, with ad libitum access to food and water. All experimental procedures were designed to minimize animal suffering, and the experimental protocol was in accordance with the Rules for Research in Health Matters (Mexican Official Norms NOM-062-ZOO-1999, NOM-033-ZOO-1995) and it was approved by the local Animal Care Committee.

To induce acute SE, rats were anesthetized with isofluorane (Sofloran, PISA, Laboratories, Mexico) in 100% oxygen and they were then secured in a Stoelting stereotaxic frame with the incisor bar positioned at -3.3 mm. A hole was drilled in the rats skull, above the right lateral brain ventricle at the following stereotaxic coordinates relative to bregma: AP -4.1 mm, L -5.2 mm, V 7 mm. A single dose of pilocarpine hydrochloride (2.4 mg in a total volume of 2 μl; Sigma-Aldrich, USA) was injected using an injection pump that was attached to the stereotaxic frame (flow 1 μl/min; Stoelting Co. IL. USA), after which the animals were returned to their cages for observation and scored according to the Racine scale [8]. Animals with a score of 4/5 were considered to have developed SE. After 90-120 minutes, SE was abolished by injecting diazepam (5-10 mg/kg,

i.p.) in order to prevent the animals death and when necessary, a second dose of diazepam was administered.
The electrophysiological data obtained in two animals was used in the present study. These animals were anaesthetized with isoflurane in 100% oxygen and positioned in a stereotaxic frame such that lambda and bregma were in the same horizontal plane. Fixed recording microelectrodes, four pairs of tungsten wires (60 μm in diameter) with a vertical tip separation of 1.5 mm, were implanted bilaterally at symmetrical locations in the posterior hippocampus (CA1, AP, -5.0 mm relative to bregma; ML, 5.0 mm; DV, -5.5 mm) and anterior hippocampus (Dentate Gyrus DG, AP, -3.5 mm; ML 2.00 mm; DV -4.0 mm). The microelectrodes were attached to a pin connector and fastened to the skull with dental cement. After a week of recovery, the rats were allowed to move freely and their behavior was recorded. Five 4-channel MOSFET small amplifiers were placed on the cable connector to eliminate movement artifacts, and the electrical activity in the hippocampus was recorded using a 7D polygraph with eight amplifiers (Grass Technologies, RI, USA) and a wide-band (0.1-3 kHz). The sensitivity was 75 μV/cm per channel and a 5 kHz/channel sampling rate was used with 12 bit precision. Experiments were performed using an iMac A1048 (Apple, USA) and MP150 software (BIOPAC Systems, CA, USA). Matlab (MathWorks) routines were used to analyze the signals [9]. Every electrode signal accounts for the electrical activity of a population of neurons in a vicinity of the implanted microelectrode.

3 Signal Analysis

The complete recording of a representative experiment is showed in Figure 1. There are four signals, from top to bottom: right DG, right CA1, left DG and left CA1.

It is defined status epilepticus as self-sustained seizure activity. There are two important things to notice in Figure 1; the first one is that SE begins in the right hemisphere a few minutes after administration of pilocarpine in both DG and CA1, nevertheless in the left hemisphere SE starts almost an hour later, this is because injection was administrated on the right lateral ventricle (see Experimental setting). The second issue is that SE ceases in the four channels approximately in the time 10000 seconds .

A frequency analysis of the signal was carried out, Fourier transform was applied to selected segments of the signal to obtain their main frequency components in order to get information for the design of the model. The main frequency components in three different segments of the recording, corresponding to basal activity, and SE activity is shown in Figure 3.

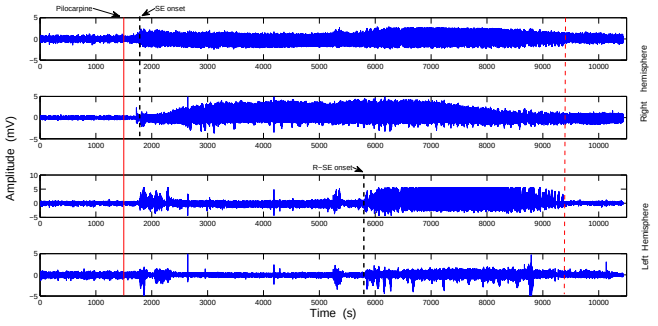

Fig. 1. Complete recording of the experiment, from top to bottom are shown the right Dentate Gyrus, right CA1, left Dentate gyrus and left CA1. The Figure shows four vertical lines, from left to right, the first (red) indicate the time when pilocarpine was administrated, the second line (black dashed) indicate the time of status epilepticus onset in the right hemisphere, the third line (black dashed) show the time of status epilepticus onset in the left hemisphere, the fourth vertical line show the moment of SE cessation

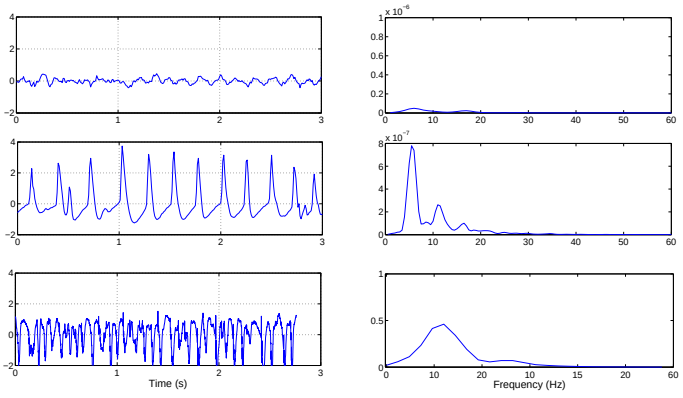

Fig. 2. Three representative types of activity (left) and their respective frequency spectrum (right) are shown. The upper sub-plot shows basal activity before pilocarpine injection and the other two sub-plots show different types of activity during status epilepticus.

4 Neural Mass Models

The present study propose to model real data obtained from intracranial EEG recordings of experimental rats by using the neural mass model methodology [10–12]. This methodology (also known as population model) allows to represent local field potentials (LFP) as the result of the interaction among populations of neurons, where some populations are formed by purely excitatory neurons and other populations are formed by purely inhibitory neurons. Then, it is combined the neural mass models with the CKF [6] to estimate in real time the states and parameters of the model with the real data. We assume that certain parameters of the model are time-varying and that is the variation of these parameters that eventually lead to epileptiform discharges. Recent studies have analyzed how certain parameter variation affects the model behavior, some of these studies have been carried out from a theoretical approach in the frame of bifurcation of dynamical systems. On other studies, more detailed models have been used and compared to real data with good results, nevertheless, estimation of parameters is done off-line with genetic algorithms. In [13] authors use a Bayesian approach and dynamic causal modelling to estimate effective connectivity among populations using FMRI time series, in [14] the CKF is utilized to estimate states of an FMRI model.

Neural mass models represent field potentials on a local area of the brain, in our case in an area adjacent to the implanted microelectrodes. It is assumed that the produced signal is the result of interacting neural populations, in specific excitatory and inhibitory populations [5]. The model can be visualized as formed by three principal components, the external input which represents activity coming from other areas (populations) of the brain, this input is usually represented by random noise. The second component is the populations of neurons presented in that particular area whose average membrane potentials are modeled by differential equations as a function of the population firing rates. The third component is the output of the model which is a combination of the states of the model. In Figure 4 a generic scheme of a neural mass model is shown, $p(t)$ is the external input, the main excitatory population is delimited by a dashed oval, the inhibitory population is depicted at the bottom delimited by a dashed rectangle, and a secondary excitatory population appears at the top of the figure. Each rectangular block with the text $h(t)$ accounts for an impulse response block whose inputs are firing rates and its output is a postsynaptic potential (similar as dendrites that receive excitatory or inhibitory synapses and transform them in postsynaptic membrane potentials). These blocks carry out a convolution between the incoming action potential sequence, i.e. firing density [15] and synaptic impulse response function, the result are postsynaptic potentials that are summed linearly. The blocks that have a sigmoid figure inside, convert the postsynaptic potential values to a pulse density i.e the firing rate of the population, through a nonlinear sigmoid function [16, 17].

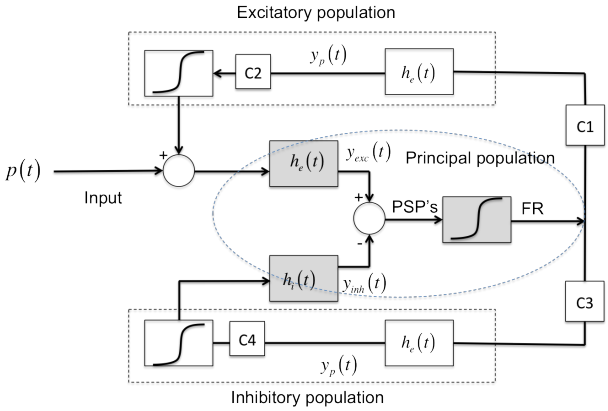

Fig. 3. Schematic representation of a general population model schematic, rectangles with the letter h_x represent the conversion from pulse density to postsynaptic potentials and rectangles with a sigmoid figure inside represent the nonlinear conversion from postsynaptic potentials to pulse density. PSP is postsynaptic potentials, FR is firing rate.

The synaptic impulse response can be represented by a second order differential equation as

$$\begin{aligned} \dot{y} &= z \\ \dot{z} &= Aax(t) + 2az(t) + a^2 y(t) \end{aligned} \tag{1}$$

where $x(t)$ is the input, $y(t)$ is the output and parameters A, a shape the synaptic response, they have different values for each neurotransmitter, i.e GABA, AMPA.
The sigmoidal function that transforms postsynaptic potential in firing rate is described by the equation

$$Sigm(y_x) = \frac{2e_0}{1 + e^{r(v - v_0)}} \tag{2}$$

where, e_0 represents the maximum firing rate, v_0 the PSP for which a 50% firing rate is achieved, and r the steepness of the sigmoidal transformation.

5 Dentate Gyrus

The DG is a cortical region that is part of a larger functional brain system called the hippocampal formation. It lies between the entorhinal cortex and the *Cornu Ammonis* area and it is thought to play an important role in preprocessing information coming from cortical areas that ultimately leads to the production of episodic memories [18]. The dentate area possess two principal excitatory cells, the *dentate granule cells* and the *mossy cells*; and at least eight types of inhibitory interneurons [19]. In the present study, it was modeled the DG as

formed by four subpopulation of neurons, the granule cells (GC) and mossy cells (MC) (both excitatory) and the pyramidal basket cells (BC) and hilar cells (HC) (both excitatory). A schematic representation is shown in figure 5, as can be observed, the inhibitory population have feedback loops which is consistent with morphological studies and this recurrent inhibitory connexion allows the model to have oscillations in the gamma band (30-70 Hz). MC connects to GC and vice-versa, BC connects principally to GC and HC connects mainly to GC and BC. The equations that describe the dynamics of the model are a modified version of Wendling and coworkers model [10] and are given by:

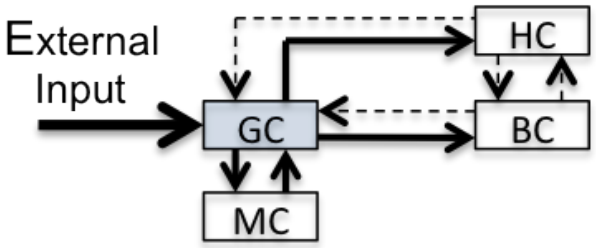

Fig. 4. Schematic draw of the dentate gyrus connection. Continuous arrows represent excitatory connections and dashed arrows represent inhibitory connections, rectangles represent population of specific types of neurons, the external input represents afferent activity from the entorhinal cortex. MC is mossy cells, GC is granule cells, BC is pyramidal basket cells and HC is hilar cells

$$
\begin{aligned}
\dot{v}_{gc} &= i_{gc} \\
\dot{i}_{gc} &= Aa(Sigm(v_{mc} - (C_4 v_{bc} + C_6 v_{hc}))) - 2a i_{gc} - a^2 v_{gc} \\
\dot{v}_{mc} &= i_{mc} \\
\dot{i}_{mc} &= Aa(p(t) + C_2 Sigm(C_1 v_{gc})) - 2a i_{mc} - a^2 v_{mc} \\
\dot{v}_{bc} &= i_{bc} \\
\dot{i}_{bc} &= Bb(Sigm(C_3 v_{gc}) - C_8 v_{hc}) - 2b i_{bc} - b^2 v_{bc} \\
\dot{v}_{hc} &= i_{hc} \\
\dot{i}_{hc} &= Gg(Sigm(C_5 v_{gc} - C_7 bc)) - 2b i_{hc} - b^2 v_{hc}
\end{aligned}
\tag{3}
$$

The states v_x are the postsynaptic potentials of the population indicated by the suffix, i.e. v_{gc} is the postsynaptic membrane potential of the granule cell population, the parameters A, B, G are the excitatory and inhibitory gain respectively, a, b, g are the lumped representation of the sum of the reciprocal of the time constant of passive membrane and all other spatially distributed delays in the dendritic network, $p(t)$ is the input to the system and represents incoming activity from external populations activity . The parameters $C_1, C_2, ..., C_8$

represent the average number of synapses from one population to other population. To be consistent with structure of DG, relations among synapses from one population to another were averaged from results reported in literature [19].

Figure 6 shows different types of activity that the model is able to reproduce and their respective frequency spectrum.

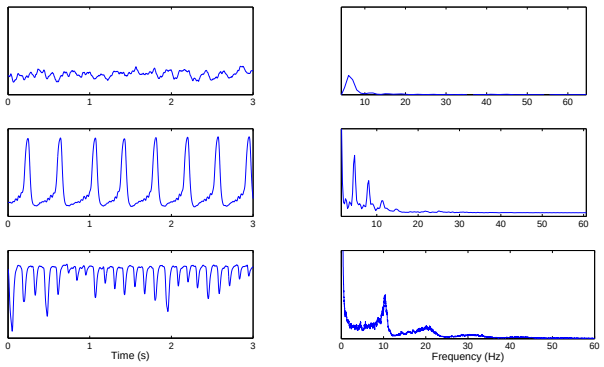

Fig. 5. three segments of simulated signals (left) and their respective frequency spectrum (right). Compare to Figure 3

For the CA1 area it was taken the model proposed by Wendling [10].

6 States and parameter estimation

Biological systems have the property of internal self-regulated environment and keep it stable. This property is called homeostasis, and it has been shown to play a central role in the regulation of normal activity within the brain [21]. In this article it was assumed that relations among internal parameters keep out the brain from experiencing and spreading seizures, but when there is a pathological condition, homeostasis fails and these relations are no longer sustained; accordingly, it is hypothesized that when estimating key parameters in the model from a real pathological signal, parameter relations should change during an ictal event. We particularly focus on three parameters, the relation on the excitation and inhibition gains [22] and the parameter K, the strength connection from a population in one area to a population in other area, i.e. from right DG to right CA1, or, from right DG to left DG. In this article estimation of states and parameters of the model was carried out with the CKF which performs efficient joint state and parameter estimation [23] and it is specially well suited for nonlinear systems [24]. Briefly, the CKF is a Bayesian, recursive predict-update process. This recursion allows for on-line estimation. In the Bayesian nonlinear

filtering paradigm it is necessary to solve integrals of the form *nonlinear function* X *Gaussian density* which are usually intractable, the CKF overcomes this issue by evaluating integrals numerically using cubature rules [6]. For a detailed explanation of the method see [14]. In general a nonlinear system can be put in terms of process and measurement equations as:

$$\begin{aligned} x_k &= f(x_{k-1}) + v_{k-1} \\ y_k &= h(x_k) + w_k \end{aligned} \tag{4}$$

where $x_k \in \mathbb{R}^n$ is the state of the system at time k, y is the measurement of the system or observed variable, v_k, w_k are zero-mean Gaussian noise and f : is a nonlinear function. The task of estimating the states of a nonlinear system consist thus in estimating x_k from only the measurement i.e. this work from the measurement are the signals from the implanted microelectrodes. Additionally to the states it is also required to estimate the parameters and the input of the system, then the parameters and input can be concatenated with the states of the system and take them as other states which evolution is described in the following way

$$\begin{aligned} \begin{pmatrix} x_k \\ p_k \\ u_k \end{pmatrix} &= \begin{pmatrix} f(x_{k-1}) + v_{k-1} \\ p_{k-1} + \xi_{k-1} \\ u_{k-1} + \gamma_{k-1} \end{pmatrix} \\ y_k &= h(x_k) + \omega_k \end{aligned} \tag{5}$$

here, p is the parameter vector and u represents the input to the system. This method is known as joint state and parameter estimation. Since epilepsy is believed to be the result of imbalance between excitation and inhibition [25], in this work we choose to track the changes in the ratio between parameters A, B and G that can be thought as the amount of excitation and inhibition, respectively. In several studies it has been shown that an increase in excitatory postsynaptic currents (EPSC) occur in pilocarpine treated rats [26]; probably because of synaptic reorganization, axon sprouting and loss of specific types of interneurons, besides, in [27] it was demonstrated that extracellular changes in glutamate and GABA occur during seizures; therefore, it is reasonable to expect a change in the parameters during SE.

In this work three different experiments were carried out: in the first one, signals were generated artificially with the present model and parameters were varied during simulation; the task in *experiment 1* consisted on identifying correctly the parameters and the states of the model by using the CKF and with only the measured variable of the model and no other information. The second experiment consisted on estimating states and parameters from real signals of intracranial microelectrodes recordings (see experimental setting section) and to analyze whether a change occur in the parameters during status status epilepticus and drug injection. The third experiment consisted on identifying strength coupling variation among populations in different microelectrode locations; especial emphasis was put on populations from opposite hemispheres.

7 Results

Next, the results from the three experiments carried out in this work are shown.

7.1 Experiment 1

In this section parameter A was varied during the simulation. The variation in this experiment is not intended to have a biological meaning but to observe the performance of the method and the behavior of the model to variations of the parameter A. In Figure 7 it is shown estimation of the output and state v_gc. It is important to notice the variation of the parameter, from time 0–20 s the parameter was varied in a sinusoid like manner, after that abrupt changes in the parameter were induced. As can be observed from Figure 8, the estimator is capable of tracking this time varying parameters. It is equally important to remark that the system undergoes a bifurcation during this parameter variation which resembles a transition from interictal to ictal state.

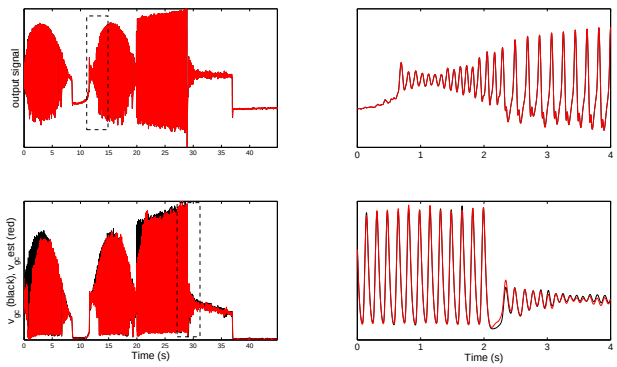

Fig. 6. Simulated and estimated signals

7.2 Experiment 2

In this experiment, the states and parameters of the neural mass model are estimated from real electrophysiological signals from microelectrodes implanted in experimental animals with temporal lobe epilepsy induced by pilocarpine. The goal was to analyze changes in the parameter during transition from interictal to ictal activity presented in SE as well as analyze changes in the parameters as a result of the transition from ictal to interictal acticity. Figure 8 shows the evolution of the estimated parameters during all the experiment. As can be observed from the signal, parameter A (excitation gain) presented low variation before

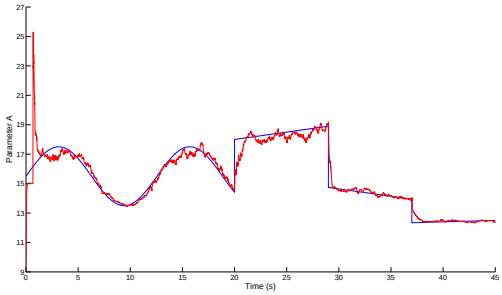

Fig. 7. Parameter estimation

pilocarpine injection, after pilocarpine at time 1300 s, parameter A presented greater variations, the higher value reached by parameter A is during SE. It is interesting to observe that at time 8000 seconds parameter A reaches its lowest value, just before SE finished. In the bottom sub-plot (Figure 9), parameters B (blue) and G (red) are shown. As it can be observed, the value of parameter B augmented during SE, perhaps in an attempt to regulate activity and parameter G increased after pilocarpine injection, perhaps this reflects the fact that during the time from 2500 to 5000 seconds there was no seizure activity even when pilocarpine was already administrated, considering homeostasis phenomena.

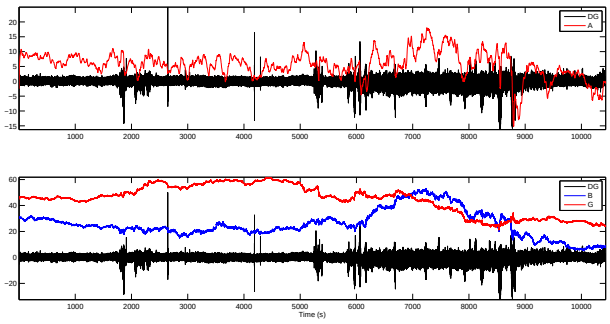

Fig. 8. Results from experiment 2. Parameters A, B and G are simultaneously estimated from a real signal. In the upper sub-plot parameter A is shown in red while the signal from the microelectrode is shown in black, scale from the real signal was modified for comparison. In the lower sub-plot parameter B (blue) and G (red) are shown

7.3 Experiment 3

Another characteristic of epilepsy is that populations of neurons can synchronize even over long distances or separate hemispheres, it has been reported that a possible mechanism for such synchronization is the strengthened coupling between neurons in distant populations; in this work it was analyzed changes in a coupling parameter between populations when signals were taken from two different microelectrodes. For this experiment two populations were modeled as coupled by a parameter K [28]. Figure 10 shows parameter K from right DG to left DG. In this case the coupling is modeled with a delay as in . Coupling between two populations increased during propagation of seizure activity to the left hemisphere even when in the right hemisphere, seizure activity started earlier.

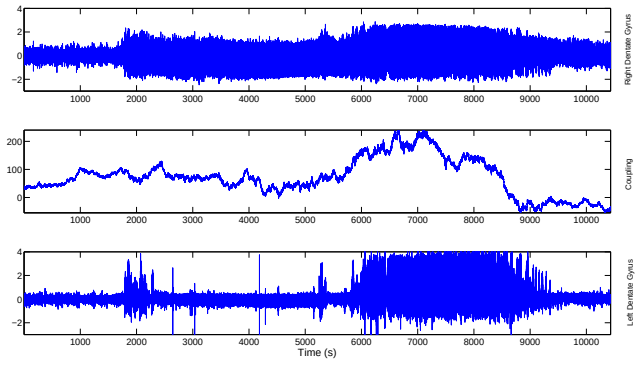

Fig. 9. Result from experiment 3. The middle sub-plot shows the estimated parameter K, the upper and lower sub-plots shows the signal from right DG and left DG respectively

8 Conclusion

Estimation of the states and parameters of a neural mass model simulated and during real intracranial EEG recordings obtained during SE induced by pilocarpine was carried out in this work. This estimation is based on the cubature Kalman filter which is specially well suited for nonlinear systems. Both, synthetic and real data was utilized in the experiments. It is worth to notice that this method can be implemented in real time, this is particularly important for the design of stimulation devices that attempt to stop seizures. The use of a neural mass model could allow for designing feedback control strategies that can deliver electrical stimulation or anti-epileptic drugs on an optimal way [29]. When estimating the parameters of the model related to excitation it was observed that during basal activity (before pilocarpine) the parameters did not

varied too much and stayed around certain value, while during ictal activity, the parameters presented a larger variation and oscillatory type behavior, as expected excitation gain increased during seizure activity.

Acknowledgments. This work was partially supported by the CONACYT grants BCT 127858, ALC 215648 and LMC 106179.

References

1. Engel J. Jr., 2006. Report of the ILAE classification core group. Epilepsia 47, 1558.
2. Perucca E., 2007. Development of new antiepileptic drugs: challenges, incentives, and recent advances. Lancet Neurology. 6, 793?804.
3. Goodfellow, M., Schindlerb, K., Baier, G., 2012. Self-organised transients in a neural mass model of epileptogenic tissue dynamics. NeuroImage. 59 (3), 2644–2660.
4. Lytton W., 2008. Computer modelling of epilepsy. Nature Reviews Neuroscience. 9, 626-637.
5. Jansen, B.H., Rit, V., 1995. Electroencephalogram and visual evoked potentials generation in a mathematical model of coupled cortical column. Biological Cybernetics. 68. 275–283.
6. Arasaratnam, I., Haykin, S., 2009. Cubature Kalman filters. IEEE Transactions on Automatic Control. 54, 1254-1269.
7. Medina-Ceja L., Pardo-Pea K., Ventura-Meja C. 2013. Evaluation of behavioral parameters and mortality in a model of temporal lobe epilepsy induced by intracerebroventricular pilocarpine administration. submitted.
8. Racine, R. J., 1972. Modification of seizure activity by electrical stimulation. II. Motor seizure. Electroencephalography and clinical neurophysiology. 32(3), 281–94.
9. Lpez-Cuevas A., Castillo-Toledo, B., Medina-Ceja, L., Ventura-Meja, C., Pardo-Pea, K., 2013. An algorithm for on-line detection of high frequency oscillations related to epilepsy. Computer Methods and Programs in Biomedicine. 110(3), 354–360.
10. Behnam Molaee-Ardekani, Pascal Benquet, Fabrice Bartolomei, Fabrice Wendling. 2010. Computational modeling of high-frequency oscillations at the onset of neocortical partial seizures: From altered structure to dysfunction. NeuroImage. 52, 1109–1122.
11. Zavaglia, M. Astolfi, L., Babiloni, F., Ursino, M., 2006. A neural mass model for the simulation of cortical activity estimated from high resolution EEG during cognitive or motor tasks. Journal of Neuroscience Methods. 157, 317–329.
12. David, O., Friston, K. 2003. A neural mass model for MEG/EEG: coupling and neuronal dynamics. NeuroImage. 20, 1743–1755.
13. Friston, K.J., Harrison, L. , Penny,W. 2003. Dynamic causal modelling, NeuroImage. 19(4), 1273-1302.
14. Havlicek, M., Friston, K.J., Jan, J., Brazdil, M., Calhoun, V. 2011. Dynamic modeling of neuronal responses in fMRI using cubature Kalman filtering. Neuroimage. 56(4), 2109?2128.
15. Lopes da Silva, F., Blanes, W., Kalitzin, S., Parra, J., Suffczynski, P., Velis, D. 2003. Dynamical Diseases of Brain Systems: Different Routes to Epileptic Seizures. IEEE TRANSACTIONS ON BIOMEDICAL ENGINEERING. 50(5), 540–548.
16. Freeman, WJ. 1987. Simulation of chaotic EEG patterns with a dynamic model of the olfactory system. Biol Cybern 56, 139–150.

17. Wilson, H., Cowan, J. 1972. Excitatory and inhibitory interactions in localized populations of model neurons. Biophysical Journal. 12.
18. Amaral, D., Scharfman, H., Lavenex, P. 2007. The dentate gyrus: fundamental neuroanatomical organization (dentate gyrus for dummies). Prog Brain Res. 163, 3–22.
19. Morgan, R, Soltesz, I. 2008. Nonrandom connectivity of the epileptic dentate gyrus predicts a major role for neuronal hubs in seizures. PNAS. 105, 6179–6184
20. Marucci G, Rubboli G, Giulioni M. 2010. Role of dentate gyrus alterations in mesial temporal sclerosis. Clin Neuropathol. 29(1), 32–5.
21. Chakravarthy N, Tsakalis K, Sabesan S, Iasemidis L. 2009. Homeostasis of brain dynamics in epilepsy: a feedback control systems perspective of seizures. Ann Biomed Eng. 37(3), 565–85.
22. Wendling, F., Bartolomei, F., Bellanger J., Chauvel, P. 2002. Epileptic fast activity can be explained by a model of impaired GABAergic dendritic inhibition. European Journal of Neuroscience. 15, 1499–1508.
23. Togneri, R., Deng, L. 2003. Joint State and Parameter Estimation for a Target-Directed Nonlinear Dynamic System Model. IEEE TRANSACTIONS ON SIGNAL PROCESSING, 51(12), 3061–3069.
24. Lpez-Cuevas, A. Castillo-Toledo, B. Medina-Ceja, L., Ventura-Meja, C. 2011. Nonlinear Identification of epileptiform signals using an artificial neural network trained with the cubature Kalman filter. IEEE World Congress on Engineering and Technology (CET), Shanghai 2011.
25. Engel J Jr. 1996. Excitation and inhibition in epilepsy. Can J Neurol Sci. 23(3), 167-74.
26. Zhan, R., Timofeeva, O. Nadler, J. 2010. High Ratio of Synaptic Excitation to Synaptic Inhibition in Hilar Ectopic Granule Cells of Pilocarpine-Treated Rats. J Neurophysiol. 104(6), 3293–3304.
27. Morales-Villagrn A, Medina-Ceja L, Lpez-Prez SJ. 2008. Simultaneous glutamate and EEG activity measurements during seizures in rat hippocampal region with the use of an electrochemical biosensor. J Neurosci Methods. 168(1), 48-53.
28. Wendling F., Bellanger J.J., Bartolomei F., Chauvel P. 2000 Relevance of nonlinear lumped-parameter models in the analysis of depth-EEG epileptic signals. Biol Cybern. 83(4), 367-78.
29. Stacey W., Litt B., 2008. Technology Insight: neuroengineering and epilepsy?designing devices for seizure control. Nat Clin Pract Neurol. 4(4): 190–201.